CHAPTER 3

METHODOLOGY

3.1 Overview

The research methodology can be divided into three parts. Firstly, the conceptual analysis is modelled based on an impulse-based UWB system and its reconfigurations and parameter settings. The analysis results are used to develop a novel adaptive impulse-based UWB system that is coded and tested by using MATLAB Simulink with IEEE802.15.3a and OMNET++ MIXIM with IEEE802.15.4a, Secondly, the proposed model is evaluated in real-time Digital Signal Processing (DSP) for UWB with additive white Gaussian noise (AWGN) and multipath fading channel models. Thirdly, the proposed model is simulated and tested as a network of nodes under different UWB channel models and communication scenarios.

This chapter describes the proposed system specifications and methodologies used in the mathematical modelling of generated impulse-based UWB signals and in the modulation, coding and shaping of pulses to generate the transmitted signal. This mathematical model is also extended to describe the IR-UWB receiver (TH-PPM receiver) in the AWGN channel and the structure of the receiver that is described as a rake receiver in the multipath fading channel model. A link budget analysis is performed to define the communication link parameters and their fixed and tunable values, which are used to formulate an IR-UWB-adjustable solution to address the changes in certain channel conditions or to satisfy certain application requirements. The performance of the communication link is evaluated over an AWGN channel model across different distances and data rates. A trade-off function that evaluates the

BER performance in different scenarios can be defined as a function between different distances, and the data rates can be defined mathematically. The mathematical modelling facilitates the design of the cross-layer architecture of the impulse-based UWB. The simulation models in Simulink are used for point-to-point communication under the AWGN channel model and for the real-time simulation of several nodes under IEEE802.15.4a channel models. The advantages of these models for the simulated implementations are also highlighted. The following flowchart in Figure 3.1 depicts the process of methodologies and the details of each block processes are explained at the rest of this chapter.

Figure 3.1: Flowchart of the proposed communication system

3.2 Research Phases in Details

Phase 1: As far as parameter choices, the generation of UWB impulse-based signal is analysed to transmit enormously short pulses with UWB

Simulations are carried out to evaluate the generated pulses in terms of various parameters for transmission, coding and pulse shaping to optimise the signal design. The analysis in this phase covers the signal at the receiver after its propagation over the radio channel. The performance of the receivers is then analysed by using different modulation techniques and channel models, especially for different rake receiver structures over simulated multipath environments. The analysis and simulation are extended to perform a UWB point-to-point template link budget analysis with different transmission parameter values.

Phase 2: This part can be described as the real-time digital signal processing (DSP) of the proposed system, which performs real-time signal generation and detection under AWGN and multipath fading channel models. The effect of IR-UWB parameter management and selection in real-time processing is determined.

Phase 3: Real-time simulation verification and qualitative comparisons of different sets of UWB communication parameters are conducted. Experiments are carried out in indoor-outdoor environments, and the system performance is evaluated under different short-range wireless communication application scenarios. The real-time simulation involves an analysis of the propagation constraints by using pulse coding variation and integration techniques, LOS and receiver filtering techniques. A functional comparison approach is adopted to achieve a meaningful comparison. Figure 3.1 presents a flowchart of the proposed communication system, and each block is explained in detail throughout this chapter.

3.3 Overview Methodology of the Proposed Solution

Figure 3.2 illustrates the settings of the UWB parameters for the data transmission and the configuration of UWB nodes that can provide the optimum performance according to their cost function. The parameters must be set in the first step, and then the QoS requirements must clearly define the throughput.

The QoS provides a long, reliable bandwidth. The UWB nodes are configured to provide optimum performance, and the data are transmitted between nodes according to their cost function and application requirements. This step aims to detect the changes in either a communication environment or in the neighbouring nodes. If changes are not detected, then the UWB nodes are reconfigured to achieve performance improvements. After the detection, the data are transmitted between nodes.

The main implementation modules are considered in the simulations conducted at different levels. The first level is the point-to-point MATLAB simulation, which evaluates the performance of the received signal across varying distances and data rate scenarios and compares such performance with that of the reference signal defined at the beginning of the simulation. At the next level of the simulation, a Simulink real-time simulation of the proposed system is carried out in real-time as a proof of concept. The implementation is extended to the third level, which is conducted in MIXIM-OMNET++ simulator environments for networks of nodes across different distance and data rate scenarios.

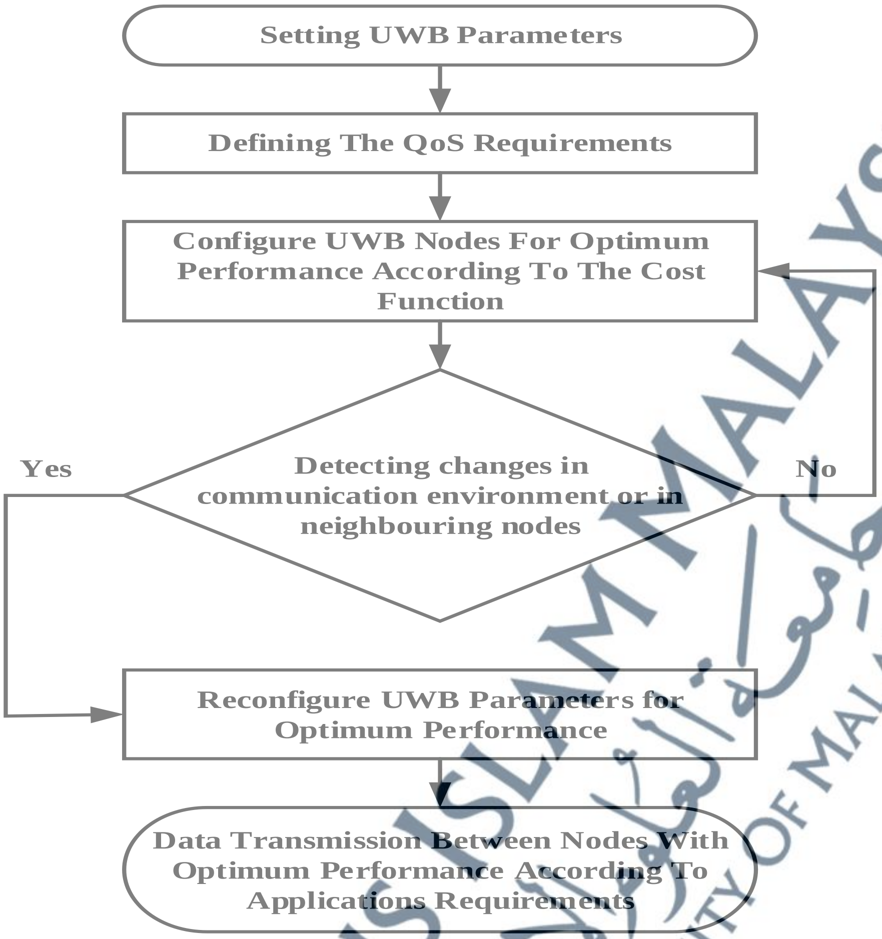

Figure 3.2: Research Design

3.4 Processes Of The Adaptive IR-UWB Template From The Proposed Communication Specifications

The proposed reconfigurable IR-UWB solution is designed as a link-template that contains all the fixed and reconfigurable parameters of signal transmission, propagation and detection. To validate this solution, its performance in terms of BER and SNR is evaluated under different simulated channel models and scenarios with different data rates. The performance of this solution is also evaluated in terms of its throughput efficiency across different data rate and distance scenarios.

3.4.1 Signal Generation

Short pulses are used for emitting UWB signals by using impulse-based UWB. To produce short pulses, the first and second derivative Gaussian functions have been recently used. The generated pulse shape signals are easy to emit and have a direct current zero offset. The pseudo-noise (PN) coding technique is frequently applied for the spread spectrum as it allows for a multiple access performance.

3.4.1.1 Transmission of the Generated Impulse-Based UWB Signal

To clearly define parameters of the generated TH-PPM pulses signal, it is good to start from the time-frame of the generated signal as shown in figure 3.2. then,the following figures showed clearly how the signal generated step by step.

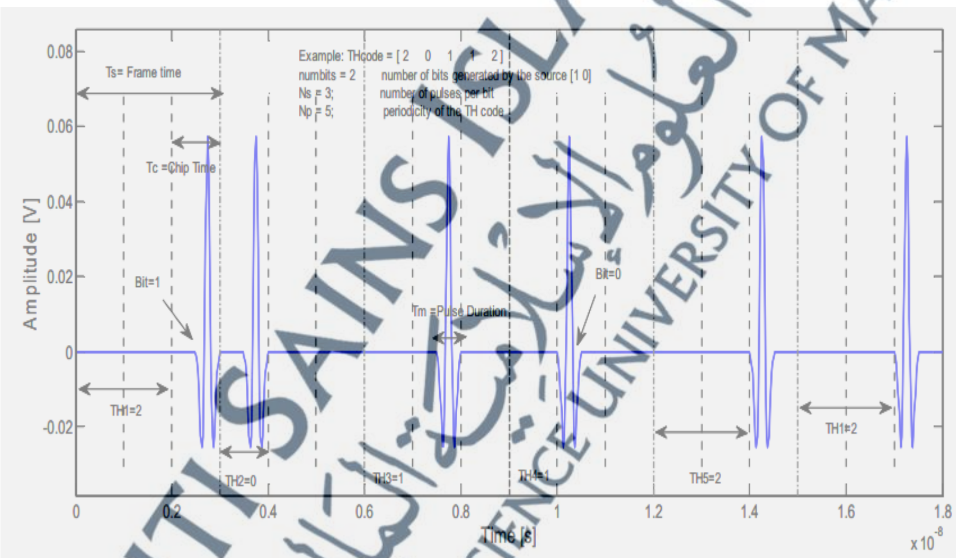

Figure 3.2: 2PPM-TH with Pulse Shape.

The process of generating the final UWB signal involves various numbers of blocks.

The first block is the code repetition coder, which is illustrated in Figure 3.3. A binary sequence b is generated as input at the rate of $R_b = \frac{1}{T_b}$ to produce a sequence where each bit is repeated N_s times. The binary sequence is generated at a rate of

$$R_{cb} = \frac{Ns}{T_b} - \frac{1}{T_s} \tag{3.1}$$

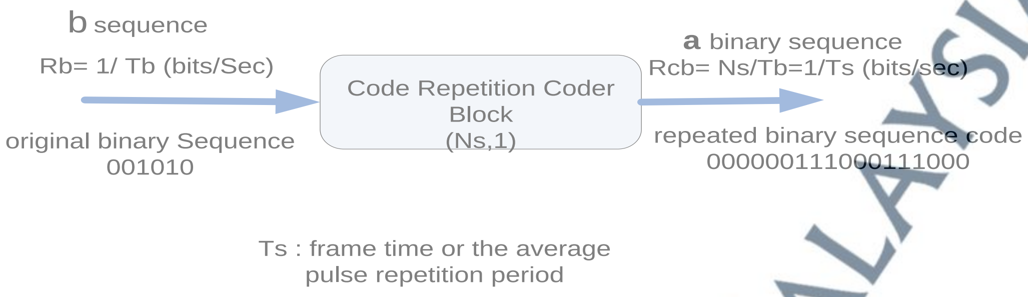

Figure 3.3: Code Repetition Coder Block

Where Ts (frame time) denotes the repetition period of the mean pulse, redundancy is introduced in this block as represented by (Ns,1). For instance, the binary sequence 001010, when passing through the code repetition block, produces a sequence ‘a’, which is the repeated binary sequence code 000000111000111000.

The second block is a transmission coder block, as illustrated in Figure 3.4. This block uses as its input the sequence ‘a’ obtained from the code repetition block. An integer value c is added to ‘a’ to produce the output d. The sequence can be mathematically expressed as

$$d_j = C_j T_C + a_j \varepsilon, \tag{3.2}$$

where Tc is the chip time (1 ns) and ε is the PPM shift (0.2 ns).

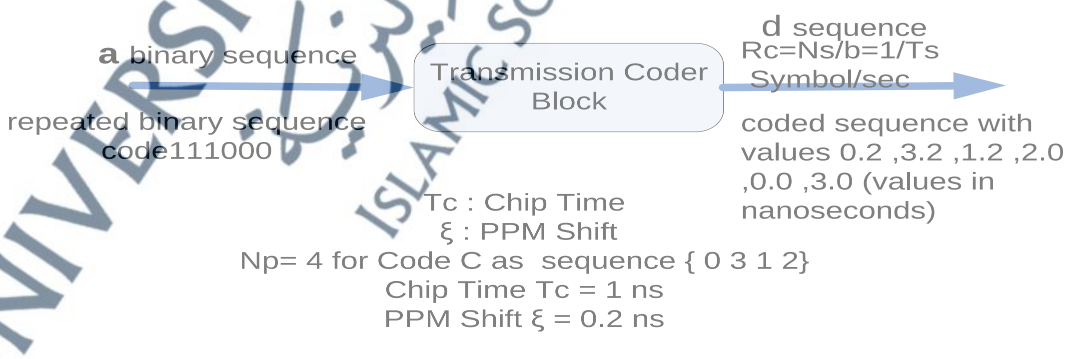

Figure 3.4: Transmission Coder Block

Both Tc and ε are constants that satisfy

$$C_j\, T_C + \varepsilon < T_s \tag{3.3}$$

For all $C_j in\ general\ \varepsilon < T_C$. Code c can be periodic with N_p, which is defined as the periodicity of the TH code.

The repeated binary sequence code 111000 is then treated as an input to the transmission coder block, and the output is the sequence ‘d’, which values are 0.0, 0.2, 1.2, 2.0, 3.0 and 3.2 in nanoseconds.

The third block is the PPM modulator, as shown in Figure 3.5. The coded real-value sequence’ is treated as the input. This block generates a sequence of unit pulses that are known as delta pulses $\delta(t)$ at a rate of $R_b = {}^{N_s}/_{T_b} = {}^{1}/_{T_s}$. The location of these pulses can be expressed at time $jTs + dj$ and shifts from the nominal position jTs by dj. Therefore, these pulses occur at time,

$$(jT_s + C_j\, T_C + a_j\, \varepsilon) \tag{3.4}$$

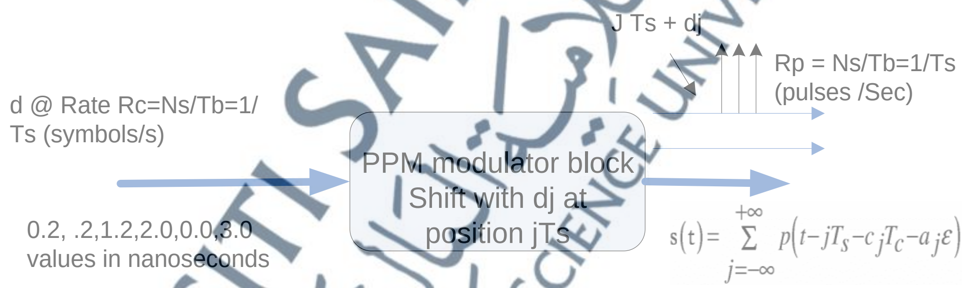

Figure 3.5: Block of PPM Modulator

The final block is the filter pulse shape (Figure 3.6), which output is the impulse response p(t). The generate signal $S(t)$ does not overlap with the pulses.

$$S\,(t) = \sum_{j=-\infty}^{+\infty} p(t - jT_s - c_jT_c - a_j\varepsilon). \tag{3.5}$$

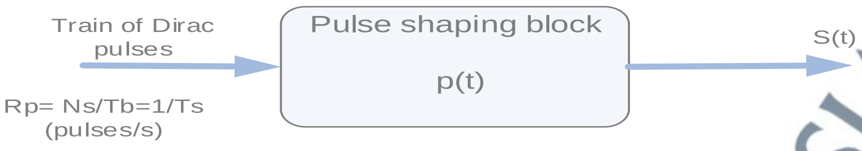

Figure 3.6: Pulse shaping block

The complete schematic of the signal generation process is illustrated in Figure 3.7.

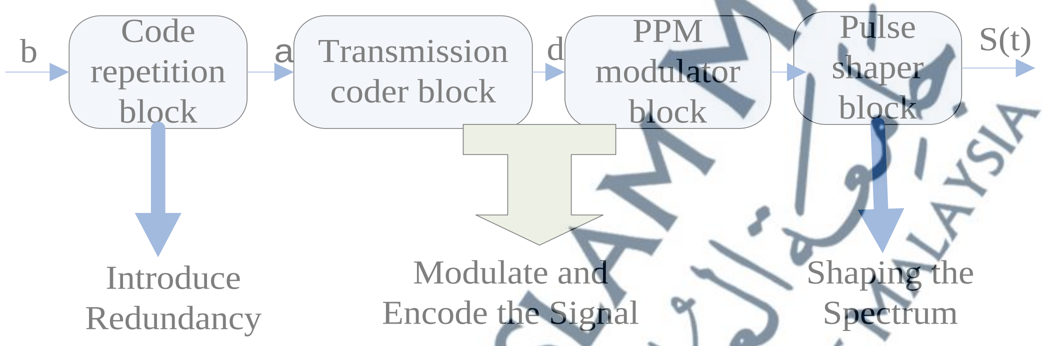

Figure 3.7: Signal Generation Process

In the following subsection, the complete transmission chain for UWB TH with PPM is simulated according to different parameter settings.

3.4.1.2 UWB Signal Shaping Processes

After defining the pulse coding and modulation in the previous section, the processes of controlling the width and shape of certain types of pulses must be described. The pulse shape is changed by modifying the pulse waveform. The bandwidth and frequency peak of the transmitted signals are affected by the impulse response of the pulse shaper. The emitted pulses have a zero DC offset. To generate a pulse shape, the bell-shaped Gaussian pulse is used.

$$p(t) = \frac{1}{\sqrt{2\pi\sigma^2}} e^{-\left[\frac{t^2}{2\sigma^2}\right]} = \pm \frac{\sqrt{2}}{\alpha} e^{\frac{2\pi t^2}{\alpha^2}} \tag{3.6}$$

where $\alpha^2 = 4\pi\sigma^2$ is the pulse shaper, and σ^2 is the variance.

By changing the α shape factor, the infinite waveform can be obtained via differentiation from the original pulse. The adopted pulse shape model is a second derivative Gaussian function Chiu et al. (2012) that can be expressed as

$$\frac{d^2p(t)}{dt^2} = \left[1 - 4\pi\frac{t^2}{\alpha^2}\right] e^{\frac{2\pi t^2}{\alpha^2}} \qquad (3.7)$$

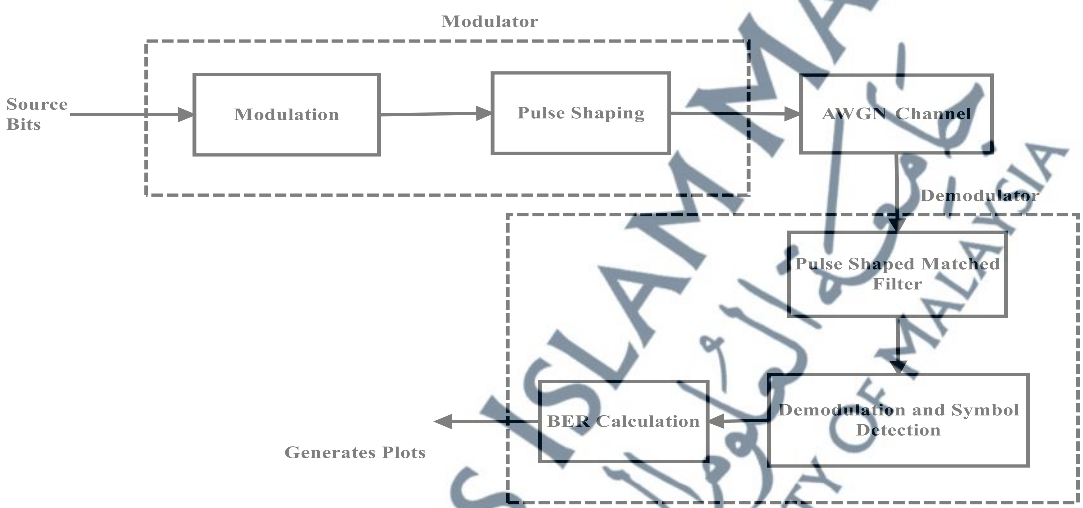

Figure 3.8: Pulse Shaping Block Diagram

The shape factor α and pulse width are directly proportional to each other. The pulse can be shortened by reducing the value of α, which allows the bandwidth to increase for the transmitted signal. By adjusting this value, the shape factor waveform can occupy various bandwidths. As shown in Figure 3.8, the source bits are used as input to the modulator, which consists of two components, namely, modulation and pulse shaping. The signal is initially subjected to modulation and is subsequently pulse shaped by changing the weights and delays. Afterwards, the signal is transmitted to the AWGN channel, which detects the useful signal that contains noise and then passes this signal to the demodulator. a demodulator has three components, namely, pulse-shaped matched filter, demodulation and symbol detection and BER calculation, and outputs the generated plots.

UWB spreads its spectrum on a large bandwidth with a high frequency. The energy of the signal when passing through a large bandwidth creates noise in the signal. UWB differs from the traditional spread spectrum as the former carries short pulses whereas the latter uses long carrier signals. The FCC has defined several UWB system characteristics that use a small bandwidth UWB-BW size with 0.20<UWB-BW<500 MHz. This small bandwidth, also known as fractional bandwidth (FB), can be computed as

$$FB=2\frac{(f_H-f_L)}{(f_H+f_L)} \quad (3.8)$$

Where the frequency range is between f_H and f_L, with f_H denoting the upper limit and f_L denoting the lower limit. The frequency in which the UWB operates ranges from 3.1 to 10.6 and the bandwidth can extend up to 7500 MHz. In contrast to intentional radiators, UWBs must produce non-damped waveforms to meet the FCC regulations. Gaussian, Rayleigh and Laplacian waveforms are all non-damped waveforms that have a flat spectrum. The Gaussian waveform function can be expressed as

$$G(x)=\frac{1}{\sqrt{2\pi\sigma^2}}e^{-a^2/2\sigma^2} \quad (3.9)$$

The Gaussian pulse can be computed as

$$g(t)=e^{-\left(\frac{t}{\tau}\right)^2} \quad (3.10)$$

where τ is the decay time.

The waveform generated by using the first derivative is

$$g'(t)=\frac{d}{dt}e^{-\left(\frac{t}{\tau}\right)^2} \quad (3.11)$$

Compared with other communication systems, such as narrowband and wideband, the generated pulse waveform can be considered a series of very narrow pulses that are modulated in different positions at a certain time interval over a very wide band as depicted in Figure 3.9.

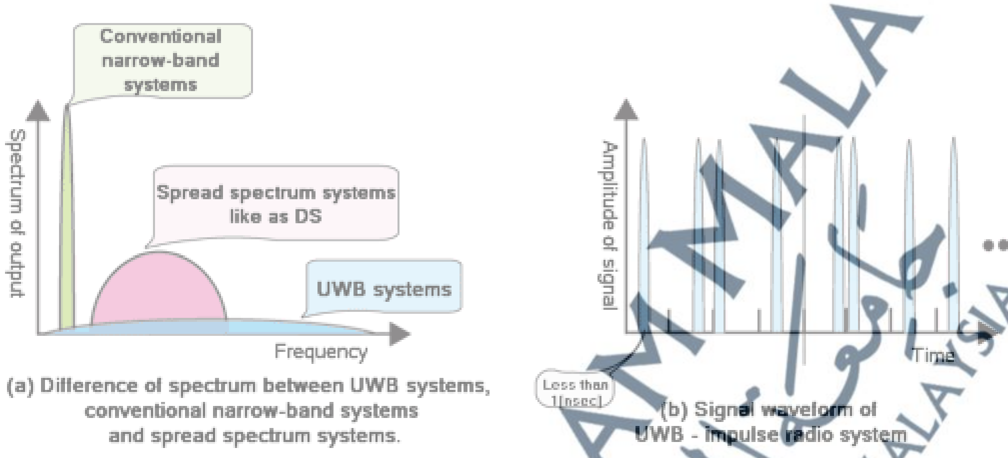

Figure 3.9: Difference Between UWB And The Traditional Spread Spectrum

The Gaussian function second derivative is also known as the Gaussian doublet. For each additional derivative, the Gaussian pulse minimises the bandwidth and increases the frequency with a constant time decay (τ).

$$g''(t) = \frac{-2}{\tau^2}\left(1 - \frac{-2t^2}{\tau^2}\right) e^{-\left(\frac{t}{\tau}\right)^2} \tag{3.12}$$

To generate a bell shape, the Gaussian pulse shape is computed as

$$p(t) = \frac{1}{\sqrt{2\pi\sigma^2}} e^{-\left[\frac{t^2}{2\sigma^2}\right]} \tag{3.13}$$

Evaluating the effect of pulse shape by varying the pulse width and changing the pulse shape in the ideal transmitter spectrum can help avoid DC components. When the narrowband intervention is reduced, a high is observed productivity in terms of BER.

The frequency-domain of the Gaussian waveform is given by

$$G(f)=\tau\sqrt{\pi}e^{-(\pi f t)^2} \quad (3.14)$$

Unlike the traditional spectrum that requires a continuous carrier signal, impulse-based UWB is carrier less. The data are encoded by using the TH BB system. The most frequently used modulation techniques in UWB include Binary Phase Shifting Key (BPSK) and PPM. The data pulse stream is encoded based on the reference pulse, and the data stream is adjusted by proceeding or postponing individual pulses in time. Given the various operating frequencies of the UWB signals, no interference is observed in the transmission line.

The impulse-based UWB system has several advantages, including its wideband radio services and non-jammed signals, by operating in different frequencies. This system also has a secure communication path. The signals are classified as follows based on their FB:

- narrowband, which has an FB range of Bf <1%,
- wideband, which has an FB range of 1%< Bf<20% and
- UWB, which has an FB range of Bf>20%. The frequency ranges of UWB are shown in Figure 3.10.

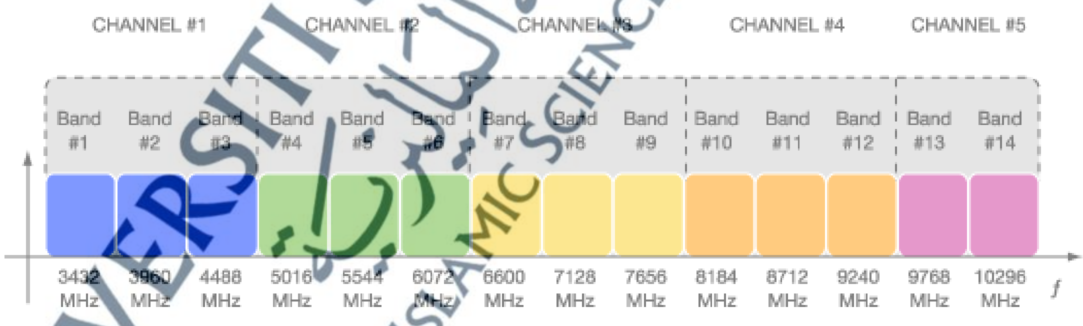

Figure 3.10: UWB Frequency Band

3.4.2 Receiver Structure of UWB TH-PPM

The AWGN signal is the simulation equivalent of the simplest random noises that occur in an environment. 'Additive' means that this signal is included in the UWB system signal, 'white' means that this signal helps operate the UWB system with a uniform power over the frequency band and 'Gaussian' means that this signal follows a normal distribution.

The receiver aims to detect the received signal that contains useful information. The generated and transmitted signal is denoted by s(t), whereas the received signal is denoted by *r(t)*. The thermal noise effect over the useful signal is considered. The received signal is expressed as

$$r(t) = \alpha\, s(t-\tau) + n(t) \tag{3.15}$$

where τ denotes channel delay, α denotes pulse shaping and $n(t)$ denotes thermal noise.

Thermal noise corrupts the waveform of the transmitted signal, and the degree of corruption depends on the ratio of the useful received energy E_{Rx} and thermal noise N_o, which proceeds in a direction opposite to that of SNR (${}^{E_{Rx}}/_{N_o}$).

As mentioned above, the transmitted signal for TH-PPM systems can be expressed as,

$$s(t) = \sum_{j=-\infty}^{\infty} p\left(t - JT_s - C_jT_C - a_j\varepsilon\right) \tag{3.16}$$

$$=\sum_{j=-\infty}^{\infty} \sqrt{E_{Tx}}\, P_o\ \left(\left(t - JT_s - C_jT_C - a_j\varepsilon\right)\right) \tag{3.17}$$

where E_{Tx} is the transmitted energy per pulse, and $P_0(t)$ is the normalised energy pulse waveform.

According to Equations (15) and (17), the received TH-PPM signal can be expressed as

$$r(t) = \sum_{j=-\infty}^{\infty} \sqrt{\alpha^2 E_{TX}}\ P_o\big(t - JT_s - \mathrm{C}_j T_C - a_j\varepsilon - \tau\big) + n(t) \tag{3.18}$$

$$=\sum_{j=-\infty}^{\infty} \sqrt{E_{Rx}}\, P_o\big(t - JT_s - C_j T_C - a_j\varepsilon - \tau\big) + n(t) \tag{3.19}$$

where $E_{Rx} = \alpha^2 E_{Tx}$ is the received energy per pulse, n(t) is the thermal noise, α is the channel gain (which is calculated as $\alpha = \frac{C_g}{\sqrt{D}^{\rho}}$, where C_g is the reference channel gain, D is the distance and set to 1 m and p is the path loss exponent) and τ is the channel delay (which is calculated as $\tau = \frac{D}{C}$, where C is the speed of light in a vacuum).

3.4.2.1 UWB Signal Propagation in Channel Models

The optimum receiver for the AWGN channel comprises a correlator and a detector. The activities of these parts are simulated to evaluate the performance of the receiver. The correlator converts the received signal into a set of decision variables, whereas the detector decides which signal waveform will be transmitted. A mathematical analysis of the aforementioned concepts is performed when the transmitter sends information in digital forms by using M different waveforms $s_m(t)$, where k = 0, …, N-1, and T is the interval duration

$$S_m(t)=\sum_{k=0}^{N-1} S_{mk}\Psi_k(t) \qquad t\in[0,T] \tag{3.20}$$

where

$$S_{mk} = \int_0^T S_m(t)\Psi_K(t)dt\,, \quad \text{with K = 0, …, } N\text{-1} \qquad (3.21)$$

According to Equation (3.20), the energy E_m of $S_m(t)$ over time T is

$$E_m = \int_0^T (S_m(t)^2 dt = \int_0^T [\sum_{K=0}^{N-1} S_m \psi_K(t)]^2 dt = \sum_{K=0}^{N-1} S_{mK}^2 \quad \forall \text{ m = 0... M -1} \qquad (3.22)$$

By introducing Equation (3.20) into Equation (3.15), the received signal in the interval [0, T] that corresponds to the transmitted signal $S_m(t)$ can be rewritten as

$$r(t) = \sum_{K=0}^{N-1} \alpha \; S_{mK}\, \psi_K(t-\tau) + n(t) \qquad (3.23)$$

The correlator receiver for r(t) in Equation (3.23) Proakis (1995) is composed of a bank of N cross templates that produce the N decision variable Z_k,

$$Z_k = \int_{\tau}^{T+\tau} r(t)\psi_K(t-\tau)dt = \alpha \; S_{mK} + n_K \;, \text{K} = 0, \ldots . \text{N} - 1 \qquad (3.24)$$

Figure 3.11 presents an example of a single signal correlator.

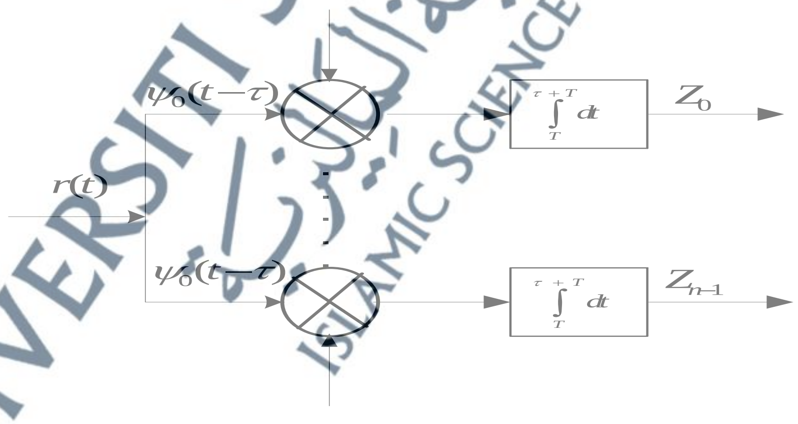

Figure 3.11: Single Correlator of A Signal

The single detector estimates the transmitted waveform based on the set $\{Z\} = \{Z_{0,\ldots\ldots,}Z_{N-1}\}$. The noise components n_k of Equation (3.24) are uncorrelated Gaussian variables with zero mean and variance Proakis (1995).

$$\sigma_n^2 = \frac{N_0}{2} \tag{3.25}$$

The signal of Equation (3.23) is generated by applying the maximum likelihood (ML) criterion. Amongst the transmitted M, the one that maximises the conditional probability p (Z| $S_m(t)$) is selected. However, $S_m(t)$, which has coefficients $S_m = \{S_{m0},\ldots..,S_{m(N-1)}\}$ closest to the set $\{Z\} = \{Z_0,\ldots\ldots,Z_{N-1}\}$, can also be selected. The following function can be derived by applying the ML criterion:

$$e((r(t),S_m) = \sum_{K=0}^{N-1}(Z_K - S_{mK})^2 = \sum_{k=0}^{N-1} Z_K^2 + \sum_{K=0}^{N-1} S_{mK}^2 - 2\sum_{K=0}^{N-1} S_{mK} Z_k = \sum_{K=0}^{N-1} Z_k^2 - 2\left(\sum_{K=0}^{N-1} S_{mK} - \frac{1}{2}\sum_{K=0}^{N-1} S_{mK}^2\right). \tag{3.26}$$

Equation (26) maximises not only P (Z | $S_{mK}(t)$) but also the correlation metric C.

$$C(r(t),S_m) = \sum_{K=0}^{N-1} S_{mK} Z_K - \frac{1}{2}\sum_{k=0}^{N-1} S_{mK}^2 = \sum_{K=0}^{N-1} S_{mK} Z_K - \frac{E_m}{2} = \int_{\tau}^{T+\tau} r(t) S_m(t-\tau)\,dt - \frac{E_m}{2}. \tag{3.27}$$

The optimum detector maximises $C(r(t), s_m)$ as shown in Equation (3.27). Figure 3.12 illustrates the roles of the correlator and detector at the receiver.

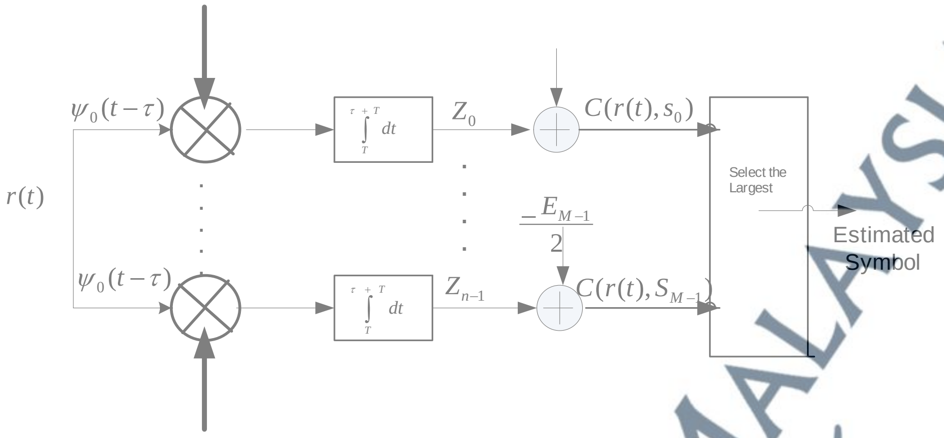

Figure 3.12: Optimum Orthogonal Binary-PPM Receiver

To achieve the optimum AWGN receiver operations, a cross-correlation for $r(t)$ is initially performed with M possible transmitted waveform $S_m(t)$, and then $E_m/2$ is subtracted from each correlation output. The maximum M value is selected. When M possible waveforms are generated, the average error probability on P_{re} denotes the probability of misdetection the symbols. An error occurs at the receiver if at least one M-1 output Z_K is larger than Z_0, the probability of which can be expressed as

$$\Pr_e = \frac{1}{\sqrt{2\pi}} \int_{-\infty}^{+\infty} \left(1 - \left(\frac{1}{2\pi} \int_{-\infty}^{y} e^{\frac{-x^2}{2}} dx \right)^{M-1} \right) e^{\left[\frac{-1}{2} \left(y - \sqrt{\frac{2E_{Rx}}{N_0}} \right)^2 \right]} dy \qquad (3.28)$$

Weeks et al. (1999)

3.4.2.2 UWB TH-PPM Rake Receiver

To simulate the performance of the receiver on the multipath channel, the UWB multipath fading channel model proposed by IEEE 802.15.3a is used for the signal propagation simulation. The channel impulse response represented in this model can be expressed as

$$r(t) = X \sum_{N=1}^{N} \sum_{K=1}^{K(n)} \alpha_{nk}\, \delta(t - T_n - \tau_{nk}) \tag{3.29}$$

Tse & Viswanath (2005)

where X is a log-normal random variable that expresses channel amplitude gain, K(n) is a number that represents the multipath contributions received by the n-th cluster, α_{nk} is the coefficient of the k-th multipath contribution for the n-th cluster, T_n is the arrival time of the n-th cluster and τ_{nk} is the delay caused by the k-th multipath contribution within the n-th cluster.

The channel can be fully characterised and represented by the impulse response of Equation (29) if the following parameters are defined:

- Λ – cluster average arrival rate,
- λ – pulse arrival rate,
- Γ – power decay factor for clusters,
- γ – power decay factor within a cluster,
- σ_{ε} – standard deviation of the fluctuation of the channel coefficient for clusters.
- σ_{ϵ} – standard deviation of the fluctuation of the channel coefficient for the pulses in each cluster.
- σ_g – standard deviation of the channel amplitude gain.

The IEEE has proposed a set of values for the above parameters, which are suitable for different IEEE multipath fading channel models across different environmental scenarios. The initial values of these parameters are tuned to fit the measurement data for these scenarios as shown in Table 3.1.

Table 3.1: Statistical Values Of The IEEE 802.15.3a Channel Model In Different Scenarios

Scenario	$\boldsymbol{\Lambda}$ **(1/ns)**	**Λ (1/ns)**	**Γ**	**γ**	$\boldsymbol{\sigma_{\varepsilon}}$ **(db)**	$\boldsymbol{\sigma_{\epsilon}}$ **(db)**	$\boldsymbol{\sigma_{g}}$ **(db)**
Case 1 **LOS (0 m to 4 m)**	0.0233	2.5	7.1	4.3	3.3941	3.3941	3
Case 2 **NLOS (0 m to 4 m)**	0.4	0.5	5.5	6.7	3.3941	3.3941	3
Case 3 **NLOS (4 m to 10 m)**	0.0667	2.1	14	7.9	3.3941	3.3941	3
Case 4 **Extreme NLOS multipath channel**	0.0667	2.1	24	12	3.3941	3.3941	3

The transmitted signal s (t) propagates over a multipath channel, and the received signal r(t) comprises the superposition of several attenuated, delayed and eventually distorted replicas of the transmitted waveform. Propagation fluctuations and path-dependent distortions can be neglected within the observation time $T \gg T_b$. The received signal r (t) can be expressed as

$$r(t) = \sum_{j} a_j S_m(t - \tau_j) + n(t) \tag{3.30}$$

where n (t) is the AWGN thermal noise effect at the receiver input.

Equation (3.29) can be rewritten as follows to reflect the statistical channel model of the UWB multipath model IEEE 802.15.3a on an impulse-based UWB received signal:

$$r(t) = X\sqrt{E_{TX}} \sum_{j} \sum_{n=1}^{N} \sum_{k=1}^{K(n)} \alpha_{nK} \alpha_j \, P_o\left(t - jT_s - \varphi_j - \tau_{nk}\right) + n(t) \tag{3.31}$$

where X is the log-normal distributed gain of the channel, E_{TX} is the energy transmitted per pulse, N is the number of clusters at the destination, K(n) is the number of multipath contributions for the n-th cluster, α_{nK} is the channel coefficient for the k-th multipath within the n-th cluster, α_j is the amplitude of the j-th transmitted pulse (such as in the case of PPM, α_j =1), T_s is the average pulse repetition period, φ_j is the time dithering associated with the j-th pulse and τ_{nk} is the delay of the k-th h path within the n-th cluster.

For simplicity, the energy for the channel coefficient α_{nK} can be normalised to unity as

$$\sum_{n=1}^{N}\sum_{k=1}^{K(n)}|\alpha_{nk}|^2 = 1 \tag{3.32}$$

and Equation (31) can be rewritten as

$$r(t) = \sqrt{E_{RX}}\sum_j \sum_{n=1}^{N}\sum_{k=1}^{K(n)} \alpha_{nK}\alpha_j\, P_o\big(t - jT_s - \varphi_j - \tau_{nk}\big) + n(t) \tag{3.33}$$

where $E_{RX} = X^2 E_{TX}$ is the total received energy for all transmitted replicas of a transmitted pulse over the multipath channel.

The detector can determine the total received energy E_{RX} when all replicas spread in time over different multipath contributions are captured. However, in practice, the detector can only analyse a finite subset of N_R contributions, and the decision implemented upon the effective energy E_{eff} is made according to the following equation:

$$E_{eff} = E_{RX}\sum_{j=1}^{N_R}\left|\alpha_j\right|^2 \le E_{RX} \tag{3.34}$$

An important factor that determines the performance and efficiency of a wireless communication system is the capability of the receiver to detect multipath energy. However, a trade-off exists between the amount of collected multipath energy and the complexity of the receiver. Rake receivers are generally used in any spreading spectrum environment to collect energy from significant multipath components. Collecting energy in rich multipath diverse environments with a certain number of receiver fingers is a common practice. A typical rake receiver comprises a bank of correlators that are sometimes referred to as fingers. Each finger is matched or synchronised with a multipath component to coherently accumulate the received multipath. One limitation of the rake receiver is that the number of multipath components that can be used and combined is limited to the power consumption, design complexity and channel estimation of the receiver. K-th numbers of delay lines are used to provide K-th replicas of the transmitted signal, and then the receiver processes the received signal to detect the signal in a K-th order diversity system. In practice, only a subset of the resolved multipath components is used by the rake receiver, and the number of multipath components determines the types of rake receivers, which are outlined as follows:

- **All rake (ARAKE):** The receiver combines and processes all multipath components.
- **Selective rake (SRAKE):** The receiver searches for the M set of the best path from all K resolved multipath components to be used as rake fingers.
- **Partial rake (LRAKE):** This receiver receives the first M arriving path from all K resolvable multipath components.

The outputs of the correlators (fingers) are merged by using the rake combiner. Different combining methods can be used, such as maximum ratio combining (MRC), wherein the amplitudes of the received multipath components are estimated and weighed in each finger. The optimal performance of MRC depends on the receiver knowledge and the channel estimation of the optimum receiver structure as shown in Figure 3.13.

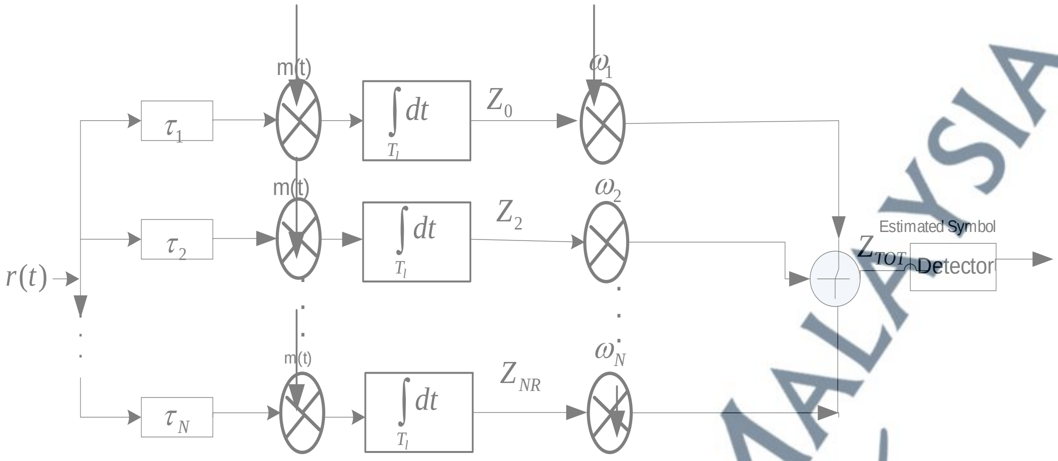

Figure 3.13: Optimum AWGN IR-UWB Receiver Structure

If $\beta = [|\beta\_0 \ , \beta\_1, \ldots . \beta\_(K-1) \ |]$, which is a set that defines rake combining weights, then this set differs according to the rake type.

- **For ARAKE (ideal rake),** combining weights is the same as combining channel fading coefficients, $\alpha = [\alpha_0 \, , \alpha_1 \, , \ldots . \alpha_{K-1}]$. Therefore, $\beta = \alpha$.
- **For SRAKE (selective rake),** the M best set of the coefficients with the largest amplitude is denoted by S. Therefore, the following weight β can be presented as $\beta = \begin{cases} \alpha_k, & k \in s \\ 0, & k \notin 0 \end{cases}$.
- **For LRAKE (partial rake),** with the M set as the first multipath component, the weighing set can be expressed as $\beta = \begin{cases} \alpha_K, & k = 0, \ldots \ldots, M-1 \\ 0, & K = M, \ldots \ldots, K-1 \end{cases}$, where $M \leq K$.

The following subsection evaluates the performance of the rake receiver over the IEEE 802.15.3a multi-path fading channel with each rake receiver structure having a different number of fingers to analyse the trade-off between receiver performance and simplicity.

3.5 UWB Channel Allocations and Channel Models

The UWB device can transmit in one or more bands following the IEEE 802.15.4a standard. These bands are classified into three levels as follows:

- sub band, with a range of 250 GHz to 750 MHz,
- low band, with a range of 3.244 GHz to 4.742 GHz and
- high band, with a range of 5.944 GHz to 10.234 GHz.

Table 3.2: UWB channels for the IEEE 802.15.4a standard

Band Group	Channel No.	Centre Frequency (MHz)	Bandwidth (MHz)	Mandatory
Sub GHz	0	499.2	499.2	Yes
	1	3494.4	499.2	No
Low Band	2	3993.6	499.2	No
	3	4492.8	499.2	Yes
	4	3993.6	1331.2	No
	5	6489.6	499.2	No
	6	6988.8	499.2	No
	7	6489.6	1081.6	No
	8	7488.0	499.2	No
High Band	9	7987.2	499.2	Yes
	10	8486.4	499.2	No
	11	7987.2	1081.6	No
	12	8985.6	499.2	No
	13	9484.8	499.2	No
	14	9984.0	499.2	No

Sixteen channels are supported in UWB PHY. The sub GHz band includes 4 low bands and 11 high bands. The channels, centre frequency and bandwidths are shown in Table 3.2. The specification of each band consists of mandatory values.

The medium used to transmit the signal from the transmitter to the receiver is the channel. Therefore, an accurate modelling of the channel must be guaranteed in UWB communication systems. A UWB system is implemented via indoor and outdoor channel modelling propagation. The indoor channel path of the UWB system model is the S-V model Radovanović et al. (2015). The indoor channel environments are classified into channel models CM1 to CM4. The IEEE 802.15.3a standard based on proliferation condition CM1 describes the LOS scenario Radovanović et al. (2015) with a large distance between the transmitter and receiver. CM1 provides the same range as CM2, but CM2 describes the NLOS scenario. CM3 falls under the NLOS medium, where the distance between the transmitter and receiver ranges from 4 m to 10 m. CM4 is an NLOS medium where the distance between the transmitter and receiver is more than 10 m. This medium exhibits a strong delay dispersion, which results in a 25 ns delay spread.

The initial set of values of these parameters is tuned to fit the measurement data for the aforementioned scenarios as shown in Table 3.3.

Table 3.3: Statistical Values Of The IEEE 802.15.3a Channel Model In Different Scenarios

Scenario	Λ **(1/ns)**	Λ **(1/ns)**	Γ	γ	σ_{ε} **(db)**	σ_{ϵ} **(db)**	σ_{g} **(db)**
Case 1 **LOS (0 m to 4 m)**	0.0233	2.5	7.1	4.3	3.3941	3.3941	3
Case 2 **NLOS (0 m to 4 m)**	0.4	0.5	5.5	6.7	3.3941	3.3941	3
Case 3 **NLOS (4 m to 10 m)**	0.0667	2.1	14	7.9	3.3941	3.3941	3
Case 4 **Extreme NLOS multipath channel**	0.0667	2.1	24	12	3.3941	3.3941	3

The channel models for IEEE 802.15.4a are specified according to their working groups. CM1 is used in residential LOS, CM2 is used in residential NLOS, CM3 is used in indoor office LOS, CM5 is used in outdoor LOS, CM6 is used in outdoor NLOS, CM7 is used in open outdoor NLOS, CM8 is used in industrial LOS and CM9 is used in industrial NLOS. The channel model is developed by using the IEEE 802.15.4a and IEEE802.115.3a standards and is subsequently parameterised.

- Indoor workplace environments: Some rooms have a similar size, but the halls are considerably large. Those areas with small offices are linked by long corridors.
- Outdoor environments: A large amount of multiple outdoor scenarios exists, and the current model includes a peripheral-like microcell scenario with a short-range.
- Industrial environments: Large enclosures filled with many metallic reflectors, which may lead to severe multipath.

3.5.1 Ghassemzadeh Path Loss Model

Ghassemzadeh proposed a numerical path loss model for the propagation of UWB signals in a PAN that is suitable for both LOS and NLOS scenarios. In this model, the path loss is estimated as

$$\mathrm{PL(d)} = [PL_0 + 10_{\gamma} log_{10} \frac{d}{d_0}] + S(d), d \geq d0 \tag{3.35}$$

Where PL0 is the calculated path loss, d0 is equal to 1 m, S is the shadow fading (log-normal) and γ is the path loss exponent. The random variables of the path loss model are denoted by γ, and the standard deviation is denoted by σ. The channel model parameters are summarised in Table 3.4.

Table 3.4: Channel Model Parameters

Parameters	Description
PL0	Path loss at d0
σγ	Standard deviation of the path loss exponent
μ0	Mean standard deviation of shadowing
μγ	Mean path loss exponent
σσ	Standard deviation of shadowing

UWB also has an improved channel capacity. The information is transmitted through the radio frequency spectrum, and the capacity increases along with bandwidth rather than with SNR.

$$C = BWlog_2(1 + S/N) \tag{3.36}$$

where C is the channel capacity, BW is the bandwidth in Hz and S/N is the SNR.

During the transmission of the signal s(t) in a multipath channel, the signal when received r(t) may produce distorted, delayed and attenuated waveforms. During the time of observation, the propagation of fluctuation and path-dependent distortions can be removed.

3.5.2 IEEE 802.15.4A UWB Channel Model

The channel model was proposed during the development of IEEE802.15.4a. The following environments are important for network applications and are used to parameterise the channel model.

(a) **Indoor residential environments:** These environments are critical for 'home networking' and linking different appliances, such as safety sensors (e.g. fire and smoke alarms), over a relatively small area. The building structures of residential environments are characterised by small units with indoor walls having a reasonable thickness.

(b) **Indoor office environments:** Some rooms in such environments are comparable with those in residential environments in terms of size, but other rooms (especially cubicle areas and laboratories) are considerably large. Those areas with many small offices are typically linked by long corridors. Each office typically contains furniture and bookshelves on the walls, which add to the attenuation provided by the (often thin) office partitions.

(c) **Outdoor environments:** Although a large number of outdoor scenarios exists, the channel model only covers a suburban-like microcell scenario with a small range.

(d) **Industrial environments:** These environments are characterised by large enclosures (e.g. factory halls) that are filled with many metallic reflectors that may lead to severe multipath.

The distance dependence of path loss is expressed in dB as

$$\mathrm{PL(d)} = \mathrm{PL0} + 10nlog_{10}\left(\frac{d}{d_0}\right) \tag{3.37}$$

Where the reference distance d0 is set to 1 m, and PL0 is the path loss exponent. The path loss also depends on the environment regardless of whether a LOS connection exists between the transmitter and receiver. Tables 3.5 and 3.6 present the key parameters of IEEE802.15.4a statistical models.

Table 3.5: Key Parameters Of IEEE 802.15.4a Residential And Indoor Office Models

Parameter	**Description**	**Residential**		**Indoor Office**	
		LOS CM1	NLOS CM2	LOS CM3	NLOS CM4
PL_0	Path loss (dB)	-43.9	-48.7	-36.6	-51.4
n	Path loss exponent	1.79	1.63	1.63	3.07
σ_s	Shadowing standard deviation	2.22	3.51	1.9	3.9
L	Mean number of clusters	3	3.5	5.4	1
$\Lambda(1/ns)$	Inter-cluster arrival time	0.05	0.12	0.016	-
$\gamma(ns)$	Inter-cluster decay constant	22.6	26.3	14.6	-
$\sigma_{cluster}$	Cluster shadowing variance	2.7	2.9	-	-
Validity	Range (m)	7-20	7-20	3-28	3-28

Table 3.6: Key Parameters Of IEEE 802.15.4a Outdoor And Industrial Environment Models

Parameter	Description	Outdoor		Industrial Environments	
		LOS CM5	**NLOS CM6**	**LOS CM8**	**NLOS CM9**
PL_0	Path loss (dB)	-43.29	-43.29	-56.7	-56.7
n	Path loss exponent	1.76	2.5	1.2	2.15
σ_s	Shadowing standard deviation	0.83	2	6	6
L	Mean number of clusters	13.6	10.5	4.75	1
$\Lambda(1/ns)$	Inter-cluster arrival time	0.0048	0.0243	0.0709	NA
$\Gamma(ns)$	Inter-cluster decay constant	31.7	104.7	13.47	NA
$\sigma_{cluster}$	Cluster shadowing variance	-	-	4.32	NA
Validity	Range (m)	5-17	5-17	2-8	2-8

3.6 Link Budget Analysis on the AWGN Channel

Link budget analysis can predict the maximum distance of propagation for a UWB communication link by using the QoS for a given data rate. The analysis is performed by monitoring the energy received over a finite time interval. The decision is made on the receiver side. The SNR of signal propagation over the AWGN channel with signal term Er and thermal noise Enoise is expressed as

$$\text{SNR} = \frac{E_r}{E_{noise}} \geq M.SNR_{spec} \tag{3.38}$$

where SNR_{spec} represents the required SNR, and M is the system margin.

The least energy required at the receiver is computed as

$$E_{r=}M.SNR_{spec}.E_{noise} \tag{3.39}$$

whereas thermal noise energy can be defined as

$$E_{noise} = \frac{1}{2} N_o = \frac{1}{2} K\ Temp_s \tag{3.40}$$

where N_o is a single-sided thermal noise spectral power density, K is the Boltzmann constant and $Temp_{SN}$ is the spot noise temperature, which is expressed as

$$Temp_{SN} = Temp_A + (F(f) - 1) \qquad (3.41)$$

where $Temp_A$ is the receiving antenna temperature, $F(f)$ is the spot noise figure and $Temp_o$ is the ambient temperature (290 K).

In the above formulations, E_r is the received signal power P_r at a finite time interval T_b. The energy received E_r can be expressed as

$$E_r = M.SNR_{spec}.\frac{1}{2}K(Temp_A + (F(f) - 1)Temp_o \qquad (3.42)$$

which is equivalent to

$$P_r T_b = M.SNR_{Spec}.\frac{1}{2}K(Temp_A + (F(f) - 1)Temp_o) \qquad (3.43)$$

The receiver power is defined as

$$P_r = 2\int_{f_l}^{f_H} \frac{P_{s(f)}}{A_{FS}} df = 2\int_{fL}^{fH} \frac{P_{s(f)}}{\frac{(4\pi)^2 D^2 f^2}{G_T G_R C^2}} \qquad (3.44)$$

where $P_s(f)$ is the double-sided PSD, and $A_{FS}(f)$ is the free-space attenuation.

Equation (3.44) can then be rewritten as

$$2T_b \int_{fL}^{fH} \frac{P_{s(f)}}{\frac{(4\pi)^2 D^2 f^2}{G_T G_R C^2}} = M.SNR_{Spec}.\frac{1}{2}K(Temp_A + (F(f) - 1)Temp_o) \qquad (3.45)$$

Based on Equation (3.45), the squared value of maximum distance D that can be covered by the transmission can be derived as

$$D^2 = \frac{\frac{G_T G_R c^2}{(4\pi)^2} 2T_b \int_{f_L}^{f_H} \frac{P_S(f)}{f^2} df}{M_S SNR_{Spec}.\frac{1}{2}K(Temp_A + (F(f) - 1)Temp_o)} \qquad (3.46)$$

Source:Proakis (1995)

From Equation (3.46), the maximum distance of the propagation can be derived for a UWB point-to-point link (P_{smin}) and target (SNR_{Spec}).

Assume that $Temp_A = Temp_o$, where the noise temperature at the receiving antenna is considered the standard temperature. This assumption is practical for terrestrial links. Equation (3.46) then becomes

$$D^2 = \frac{\frac{G_T G_R c^2}{(4\pi)^2} 2T_b \int_{f_L}^{f_H} \frac{P_S(f)}{f^2} df}{M_S SNR_{Spec}. \frac{1}{2} F_k Temp_o} \tag{3.47}$$

The modulation types that affect the relationship between SNR and P_{re} can be easily expressed as noise in the AWGN channel model. The performance of the receiver with various modulation types can be evaluated as described in the following paragraphs.

Given a target P_{re}, to evaluate the required SNR_{Spec}, the system margin is assumed to be zero for ($M_s = 0$) for simplicity. Several studies have analysed the relationship between P_{re} and SNR_{Spec} (pre-determined SNR requirement) for different UWB impulse-based modulations. The link budget analysis for M-ary PAM (M-PAM) and M-ary PPM (M-PPM) can be summarised as follows.

For M-PAM,

$$Pr_e = \left\{1 - \frac{1}{M}\right\} erfc(y) \tag{3.48}$$

Where

$$y^2 = \frac{SNR_{Spec}}{\frac{2}{3}(M^2-1)} = \frac{P_r T_b Log_2 M}{\frac{1}{2} kFTemp_o \frac{2}{3}(M^2-1)} = \frac{E_b}{N_o} \frac{3 log_2 M}{No(M^2-1)} \tag{3.49}$$

where E_b is the average bit energy, N_o is the power density in the AWGN channel, $M = 2^K$ is the number of information bits carried by each symbol and Pre is the probability of the symbol error that is used for the system specifications than for

SNR. The relationship between SNR and Pre is affected by the modulation types and is represented as noise in the AWGN channel.

The boundaries between $\frac{E_b}{N_0} > ln2$ and $E_b/N_0 > 4ln2$ for $\frac{E_b}{N_0} > ln2$ are given as

$$P_{re} < \frac{2^K}{2^K - 1} e^{-k(\sqrt{\frac{E_b}{N_o}} - \sqrt{\ln(2)})^2} \quad (3.50)$$

whereas those for $E_b/N_0 > 4ln2$ are given by

$$Pr_e < \frac{2^{k-1}}{2^k - 1} e^{-k(\frac{E_b}{2N_o} - \ln 2)} \quad (3.51)$$

The link budget for M-PAM and M-PPM is then theoretically evaluated in terms of the probability of symbol error (Pre) for specific SNRs and distances D. The experimental and simulation results are explained in full detail for validation purposes.

3.7 Trade-Off between BER and Data Rate in Various Distance Scenarios

The performance of impulse-based UWB can be analysed by using tunable parameters at the transceiver side. The transceiver is self-configured to meet the application requirements in various scenarios, such as indoor and outdoor LOS and NLOS environments. To evaluate system performance terms of BER, a dynamic reconfiguration system is designed as a cost function that is analytically formulated as follows.

- Firstly, the cost function amongst three parameters (data rate, distance and BER) is treated as a trade-off. To obtain the third variable or parameter, the other two variables can be compromised. The impulse-based UWB parameters are flexible and adjustable. The QoS threshold for BER can be transmitted at various data rates.
- Secondly, the current resource allocation for each node and the current QoS environmental conditions are examined. In this step, the node selects the

optimum modulation schemes. The configuration that needs to be done must be known prior to the system, and the configuration can reflect the system performance in terms of its modulation schemes, data rates, targeted BER and E_b/N_0.

- Thirdly, the condition of the channel is evaluated in various environments. The UWB system is reconfigured to meet the QoS requirements.

A formula, such as a local cost function, can be set in each node. The three variables (BER, data rate and distance) used to describe the performance metrics can be combined as follows in a way that any two performances metrics can be achieved at the cost of the third metric:

$$P = \frac{\text{BER*Distance}}{\text{Data Rate}} \tag{3.52}$$

where P is the performance function.

The distance can be substituted by the ratio E_b/N_o so that

$$P = \frac{\text{BER*} E_b/N_o}{\text{Data Rate}} \tag{3.53}$$

BER is a function related to m (modulation types), pulse repetition interval (PRI), E_b/N_o (average bit energy), channel impulse response h(x) and interference i(x) and is expressed as

$$\text{BER} = W\,(E_b/N_o\,, \text{PRI}, \text{m}, \text{h}\ (\text{x}), \text{i}(\text{x})) \tag{3.54}$$

E_b/N_o is a function related to the maximum distance between the transmitter and the receiver and to the maximum radiated power allowed for a given data rate, which in turn can be expressed as

$$E_b/N_o = Y\,(\mathrm{dist}, \mathrm{m}, \mathrm{PRI}) \tag{3.55}$$

The data rate depends on both m and PRI

$$\text{Data Rate} = (log_2 m)/PRT \tag{3.56}$$

The communication system performance function (P) is defined as follows by using all variables in Equations (3.53) to (3.56):

$$\mathrm{P} = \frac{PRI.w\left(E_b/N_o, PRI, m, h(x), i(x)\right).Y(dist, m, PRI)}{log_2 m} \tag{3.57}$$

As environmental conditions change, the performance cost function changes for a given probability distribution p (z), that is,

$$\bar{P} = \textstyle\sum_{\forall} P(z).P_{Previous}(z) \tag{3.58}$$

All these parameters can be determined by using a suitable cost function.

The changes in channel conditions caused by dynamic real-time environments are then detected, and IR-UWB is reconfigured for optimum modulations to meet the QoS requirements. The suitable system configurations that meet the new QoS requirements are eventually identified to allow the node to transfer data by using suitable transmission techniques of pulses in real-time environment changes.

3.7.1 UWB PHY-MAC Design for Different Applications and QoS Requirements

The proposed design architecture of the trade-off flexibility of Impulse based - UWB for different data rates and operational ranges for specific BER requirements. The BER performance in different data models and various distance scenarios can be significantly improved by following the instructions sent from the MAC layer to the physical layer to tune the generation of pulses for different physical parameters, such as modulation techniques and tuning of PRIs. This approach can directly increase the data transmission rates and the resiliency of the generated pulses to interferences, which will subsequently enhance the signal power to noise ratio and improve BER. Therefore, this approach can effectively increase the power of pulses to reach higher coverage ranges under certain channel model constraints. Figure 3.14 illustrates the proposed architecture for tuning and controlling the physically generated pulses at the physical layer by following the instructions sent from the above MAC layer to satisfy certain BER, coverage and data rate requirements.

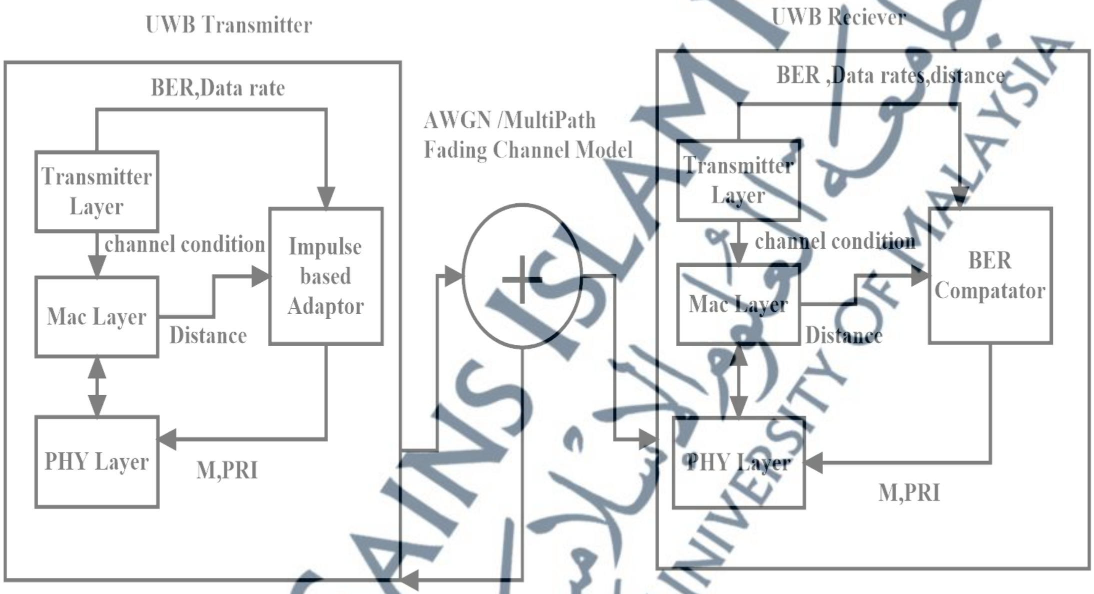

Figure 3.14: Design Of The Proposed Tuneable impulse-based UWB

The process flow of the impulse-based UWB system is shown in Figure 3.15. This process begins by setting the UWB parameters. When the UWB parameters are set at the QoS level (a BER requirement), some settings at the physical layer that are related to pulse shape and modulations can improve the BER performance by enhancing the resiliency of these pulses to interferences and by increasing the data rates of the transmitted pulses.

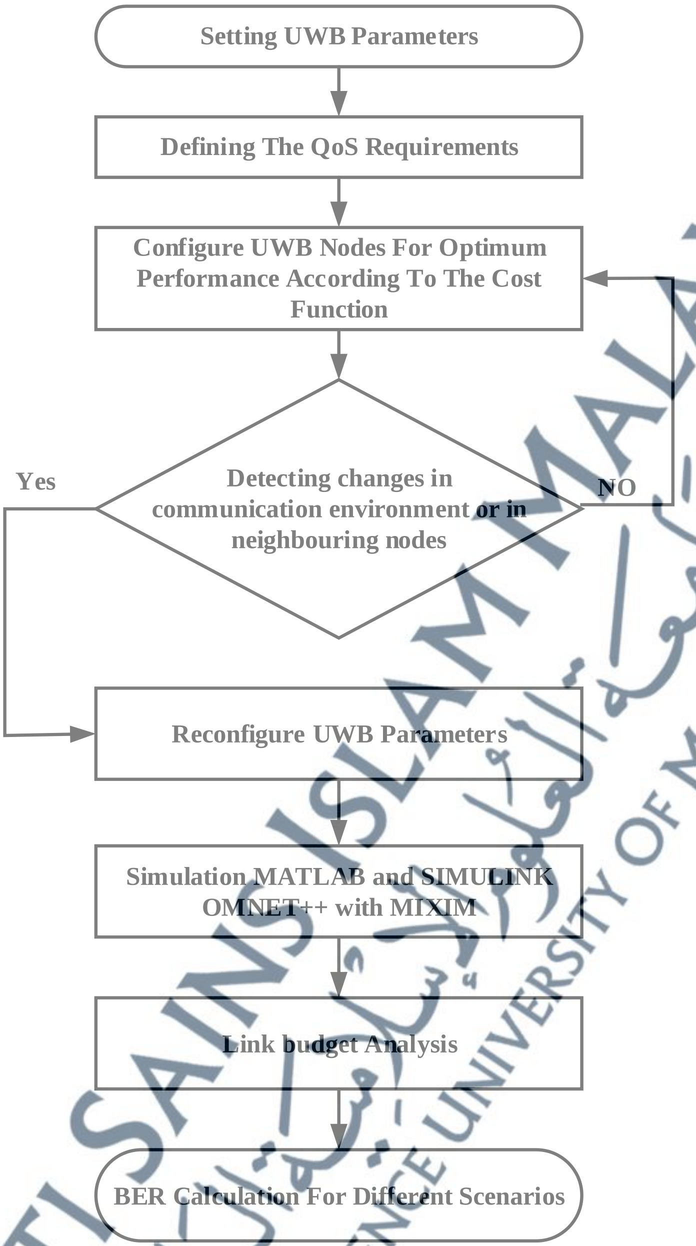

Figure 3.15: Adaptive Process Of Impulse-Based UWB

Figure 3.16 summarises the methodology for turning the PHY layer parameters in a cross-layer design according to the demands in the MAC layer and the PHY parameters that are tuned to meet the MAC layer criteria.

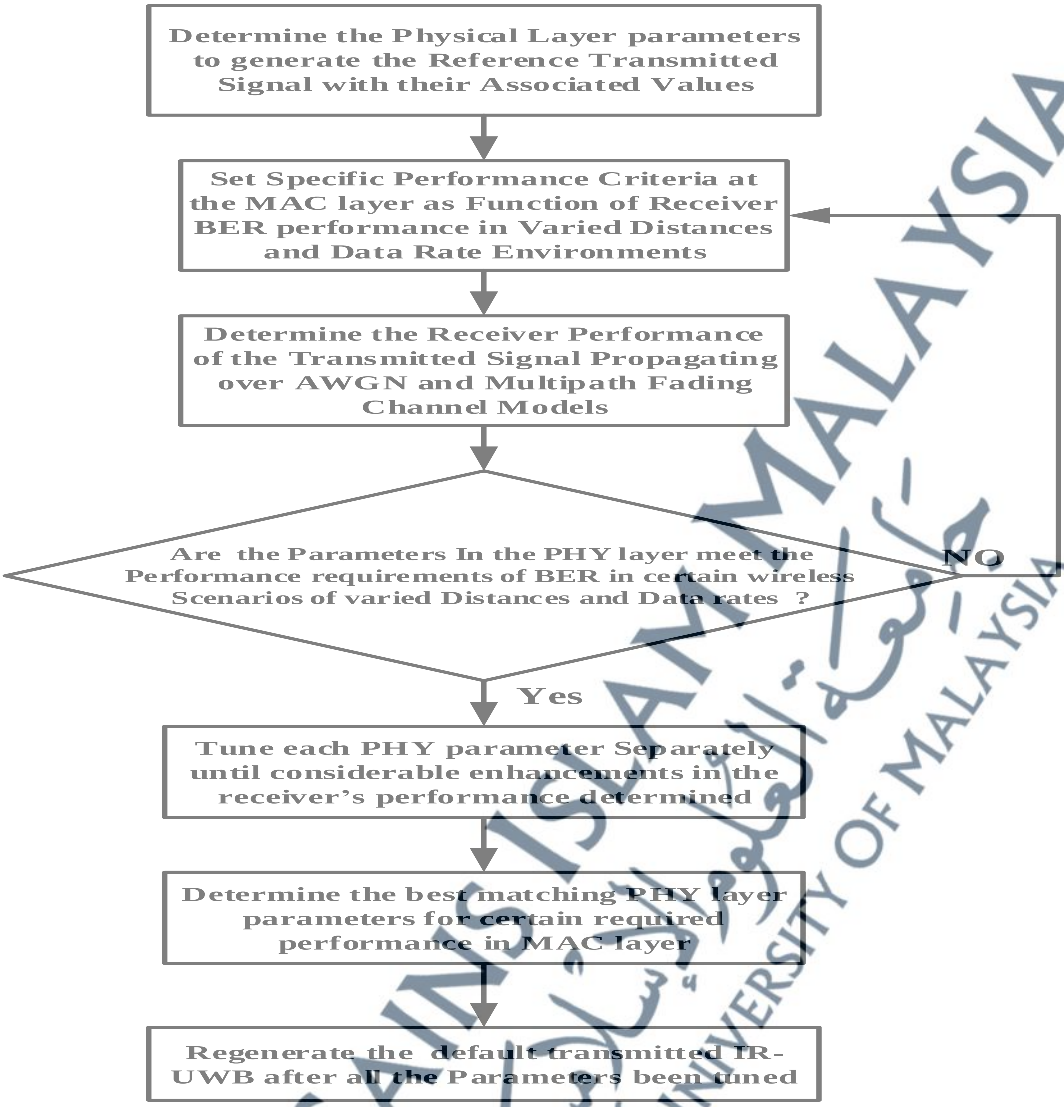

Figure 3.16: Flowchart Of The PHY-MAC Tunable Layer IR-UWB Solution To Meet Certain Application Requirements

3.8 Simulink and OMNET++/MAXIM Simulation of the Proposed UWB Architecture

The simulation model aims to assess the generation of signals with various UWB signal transmission parameters in the time and frequency domains.

- The parameters that must be adjusted to obtain an optimised solution are managed in a database that controls the transmission rate.
- Another objective of the simulation model is to examine the signal propagation channel. Like the thermal noise and the signal attenuation in the AWGN

channel model and the complex problems like transmitter effects, receiver alignment in the multipath fading.

- To examine the activities of the receiver (i.e., detecting synchronisation and demodulation).

The features of the Simulink model are summarised as follows.

- End-to-end PHY (streaming mode), which simulates and analyses different generated pulse parameters, such as pulse width, pulse modulations and pulse shaping.
- The AWGN model and multipath channel simulate the signal with the noise and deprivation consequences of LOS and NLOS multipath fading environments in different distance scenarios.
- The TH spectrum spreading technique is used along with different coding schemes, such as PPM and PAM, for data transmission.
- The fixed-point model of the UWB transceiver can be integrated into the complete software-defined radio design of a tuneable IR-UWB solution.
- Simple database management is implemented to control the generated signal parameters and data transmission rates.
- Real-time BER display.

By using the impulse-based UWB communication model (i.e. SIMULINK and MIXIM), the BER performance is validated by conducting experiments on the link budget design, which will be discussed in the next chapter. A statistical analysis of the received signal is also performed to evaluate the performance of the proposed link budget template in Chapter 4 under different scenarios.

The UWB parameters are reconfigured to determine the optimal path and BER from different channel models and scenarios. The cross-layer architecture is designed to spread the bandwidth usage according to the application requirements. The simulation model detects the changes in the neighbouring nodes and in the environment by examining the receiver. The simulation model for IEEE802.15.3a is built by using MATLAB and Simulink, whereas that for IEEE802.15.4a is built by using OMNET++/MIXIM. The communication link impulse-based UWB system is then examined. If some changes are detected in the neighbouring nodes or in the environment, then the parameters are reconfigured in the database to meet the requirements. A link budget analysis is eventually performed on the basis of the results of the simulation models. The analysis determines the gains and losses in the signal sent by the transmitter to the receiver through the channel.

3.8.1 Simulink Model Modules

The model used in the simulation has three parts, namely, the source, channel and receiver.

A. Source

- The M-ary signal source can generate pulses with different shapes (Gaussian, sinusoidal, rectangular or Manchester). The signal in this model is simulated by using the second derivative of the Gaussian signal. The Matlab code for this signal is represented as a 2nd-Gaussian.m file in Appendix A (Part 2).
- The PN code generator for the transmitter generates quasi-random PN sequences to achieve quasi-orthogonality and to protect the information carried by the transmitted signal.

B. Channel

- A channel delay, which is caused by the distance between the transmitter and receiver, is introduced. For instance, when the distance between the transceiver and the receiver is 10 m, then the channel delay is 0.33 ns. MATLAB represents this delay as a Channel-Delay.m file in Appendix A (Part 2).

- The noise introduced by the AWGN module has an average noise power of – 40 dBm. MATLAB stores this module as AWGN-Channel.m in Appendix A (Part 2).
- The IEEE 802.15.3a multipath fading channel model block is inserted into the communication model to simulate different LOS and non-LOS multipath statistical delays and to affect different distance scenarios.

C. Receiver

The receiver module has five main parts, namely, the correlator–detector, the pilot signal generator, the acquisition part, the PPM signal generator and the demodulator and integrator.

The signal is detected by using a correlation-based detector block after receiving samples of the received signal that are correlated with a known UWB signal at the receiver side. The detection is based on a threshold that is set to be equal to the pulse width time, thereby providing enough time to recover one UWB signal. The detection threshold should be high enough to avoid false UWB signal detection that will make the acquisition impossible. Figure 3.17 shows the UWB Simulink blocks of UWB signal detection.

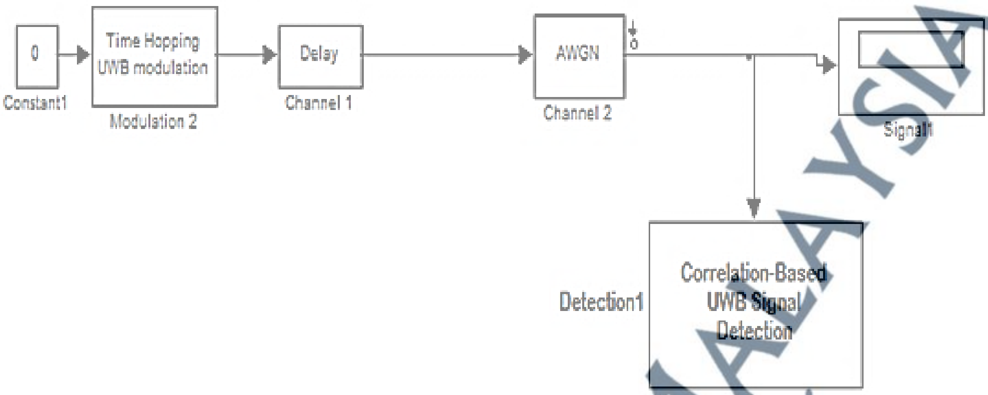

Figure 3.17: Simulink Blocks Of UWB Signal Detection

After detecting the UWB signal, both the local pilot generator and acquisition blocks start working together to determine the autocorrelation between the PN sequence and the received signal with an aim to make the pilot signal generate a UWB signal that is synchronised with the code. This process is based on a comparison between the pilot and received signals in an attempt to synchronise a PN sequence. Figure 3.18 shows the different simulation blocks for performing a successful UWB signal synchronisation.

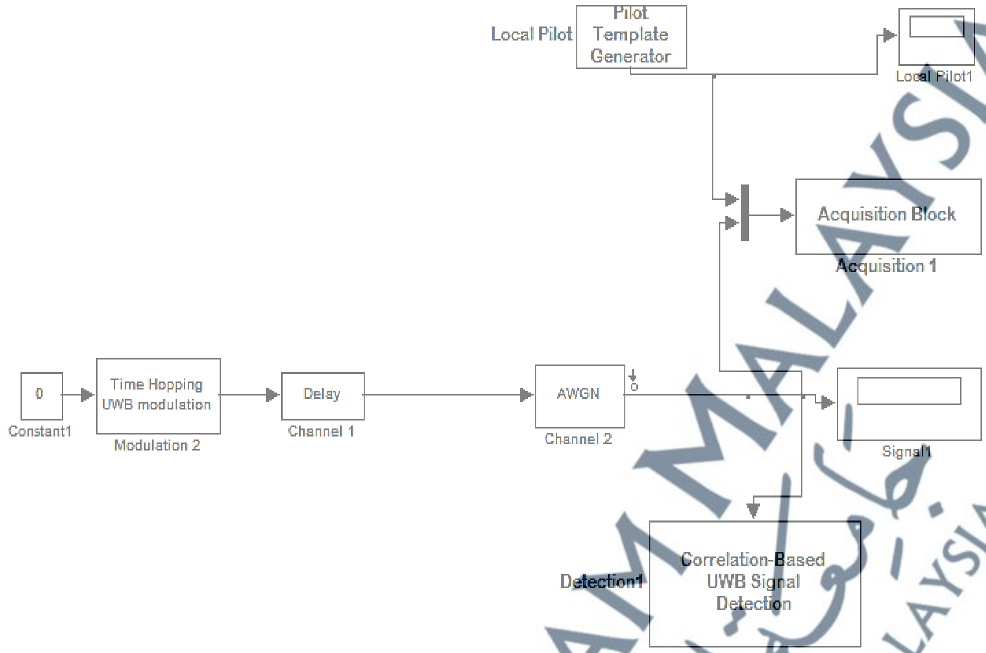

Figure 3.18: Simulink Blocks Of UWB Signal Synchronisation

The operations and interactions of these blocks are schematically shown in Figure 3.19.

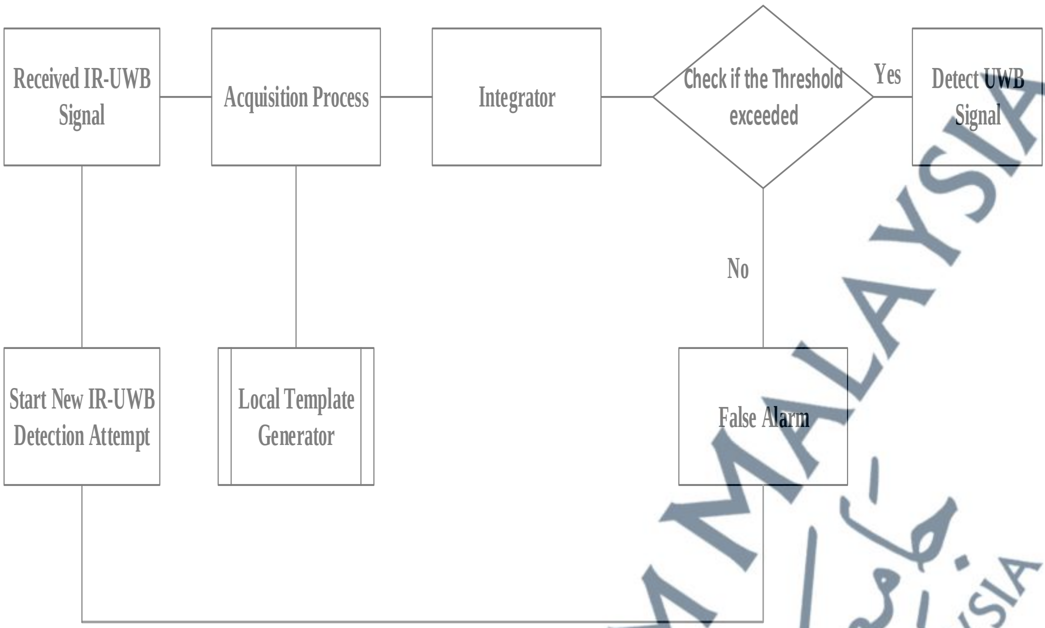

Figure 3.19: Flowchart Of Successful UWB Signal Detection

3.8.2 The OMNET++ Simulation for IEEE802.15.4a Transmitter Structure and Signal Model

Figure 3.20 illustrates the main components of an IR-UWB transmitter, according to the IEEE 802.15.4a standard.

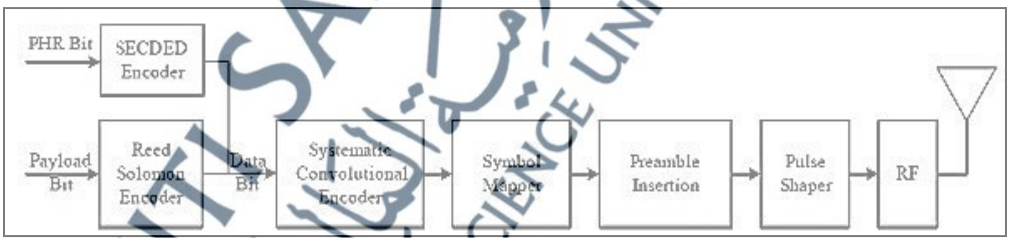

Figure 3.20: Basic Block Diagram Of An IR-UWB Transmitter According To The IEEE 802.15.4a Standard

The information bits are initially encoded by an RS encoder, which is a block error correction code that works by oversampling a polynomial generator constructed from the input data. The RS encoder takes a 330-bit block at a time and adds 48 parity bits according to a standard polynomial generator. Therefore, the RS encoder has a rate of approximately 0.87. The encoded bits are then optionally encoded by a 0.5-rate convolutional encoder.

A UWB symbol carries a pair of encoded bits. Figure 3.21 presents the structure of a UWB symbol, where the Tsym symbol duration is divided into two intervals, referred to as the Binary Position Modulation (TBPM) duration of the burst position burst of UWB pulses is transferred at each symbol interval, and the place of the burst either in the first or second intervals indicates a bit of data. In other words, if the burst is in the first half of the symbol, then ‘0’ is transmitted. However, if the burst is in the second half, then ‘1’ is transmitted. This phenomenon is referred to as BPM. The polarity of the burst carries another bit of data that corresponds to BPSK. Overall, the BPM-BPSK modulation can carry two parts of data per symbol. Specifically, one bit is used to determine the pulse burst position, whereas the other bit is used to modulate the same burst phase.

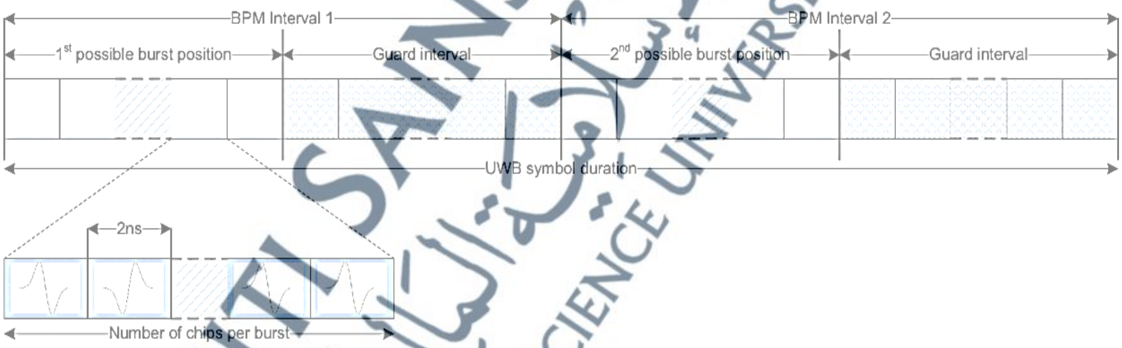

Figure 3.21: IEEE 80215.4a UWB PHY Symbol Structure

Figure 3.21 shows that the burst can be transmitted in one of many intervals, each with length Tburst, in the first or third quarter of the symbol. The position of the burst can be determined by a burst-hopping sequence, which is robust against multi-user interference.

After using the symbol mapper in Figure 3.21, a preamble is added prior to the header of each packet for timing acquisition, coarse- and fine-frequency recovery, packet and frame synchronization, channel estimation and leading-edge signal tracking for ranging. Afterwards, the bits are transmitted by using UWB pulses, pulse shaper, RF components and antennas.

3.9 Evaluation criteria

The evaluation criteria of the proposed solution can be considered as BER meeting criteria of certain acceptable range of probability of the error and not exceeding that range. This can be considered alongside with certain required range and data rates to serve the requirements of different short-ranges wireless scenarios.

3.10 Summary

This study proposes the IR-UWB cross-layer design concept with tunable and flexible parameters that can be used for generating and transmitting signals. The performance of this system is evaluated in terms of its BER and SNR in indoor and outdoor scenarios with various distances and data rates. A dedicated template of the IR-UWB communication link is theoretically evaluated to validate the proposed concept and its results. The template link design is implemented through MATLAB to check the functionality of the system. The complete system is simulated by using a real-time simulator that can change the parameters and link budget of the system to evaluate its BER and SNR. The following chapter discusses the real-time simulation, the simulation design and the system implementation in indoor and outdoor scenarios. The simulation model for IEEE802.15.3a is built by using MATLAB and Simulink, whereas that for IEEE802.15.4a is built by using OMNET++ and MIXIM. The communication link impulse-based UWB system is then examined based on these models.